Studies of Various Topologies of Passive Magnetic Current Limiter

Studies of various topologies of passive magnetic current limiter

S.C. Mukhopadhyay[a], M. Iwahara[b], S. Yamada[b] and F.P. Dawson[c]

[a]Institute of Information Sciences and Technology, Massey University, Palmerston North, New Zealand

[b]Faculty of Engineering, Kanazawa University, Kodatsuno 2-40-20, Kanazawa 920-8667, Japan

[c]Department of Electrical and Computer Engineering, University of Toronto, Toronto, Canada

Abstract. Different topological configurations for a passive magnetic current limiter consisting of a permanent magnet and saturable core are discussed in this paper. The models for a series/parallel biasing mode, and a single/three phase supply system have been fabricated and the experiments have been carried out for the performance evaluation. Using tableau method, the transient performance of different models has been simulated. The feasibility of applying the current limiter for the protection of power semiconductor devices in moderately low voltage applications is investigated.

1. Introduction

In the event of a short-circuit, fault or any other abnormal condition, a large fault current flows in power systems. The severity of this fault increases as the short circuit ratio for the system at the point of common coupling increases. Systems or devices connected in series with the fault current path are exposed to the fault current and thus the design of components must take into account the maximum anticipated fault current. Device selection is based solely on the device's surge rating at ratios of high surge current to nominal current. Thus current limiting becomes a necessity in order to reduce the rating of the component and thereby to lower the capital cost and improve protection coordination [1].

Over the last few years, the authors have been engaged in research and development of a passive type magnetic current limiter consisting of a NdFeB permanent magnet with axial magnetization, a flux directing core, a saturable core and a current winding [2–5]. The saturable core can be constructed of a ferrite, amorphous or Si-steel material or any other magnetic material having a low saturated flux density and a low saturated permeability. The combination of two such assemblies connected electrically in series but in magnetic counter opposition to each other result in a bipolar fault current limiter [2]. This limiter is placed in series between the source and the load.

2. Configurations of magnetic current limiter

The physical construction of the current limiter can be designed according to the following three criteria: biasing mode, core material, number of phases in the supply system. Each of these is discussed below.
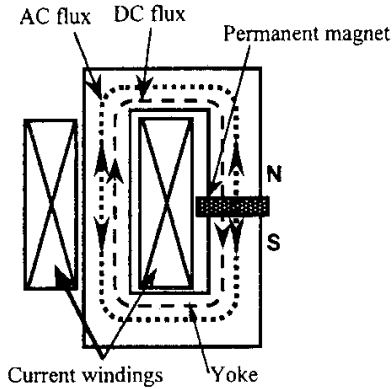
(i) Based on biasing mode

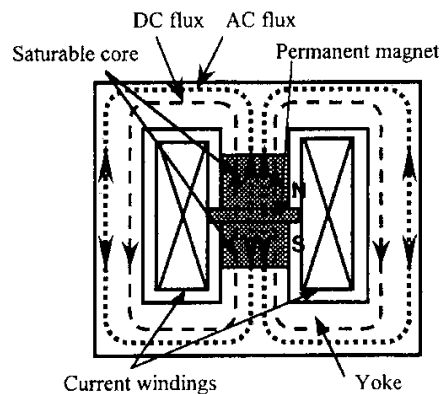Fig. 1. FCL scheme based on series biasing mode.

Fig. 2. Experimental model of FCL in series biasing mode.

The magnet can be configured either in series or parallel biasing configurations. The magnet in a series biasing configuration as shown in Fig. 1 is exposed to the magnet's dc flux and also the ac flux generated by the winding current. The disadvantage of this approach is the generation of eddy- current losses in the magnet and a potentially higher risk of demagnetization over time is inevitable. Experiments were performed on devices of small scale model fabricated in the laboratory. The device in Fig. 2 consists of two sets of ferrite C-cores placed pole to pole but separated by magnets. Hence the saturable core section and the yoke for this setup represents one continuous piece rather than separate sections. The drawback of such an approach is the soft transition between the low inductance and high inductance state.

Unfortunately due to material incompatibilities, we were not able to design the Si-steel yoke device to meet our specifications and thus the knee-point current was too low. This problem can be overcome by a suitable choice of materials and geometry.

In contrast, the magnet in a parallel biasing configuration is exposed only to the magnet's own dc flux and thus the issue of demagnetization or eddy-current losses does not play a significant role. On the other hand, the ratio of the unsaturated inductance to saturated inductance is lower and thus the let through peak current for this type of design will be higher. A schematic depiction of this approach is shown in

AC flux   DC flux   Permanent   Current
                    magnet   windings
Current
windings

N

Magnet

S

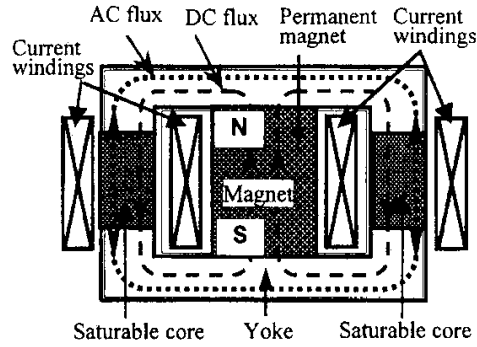Saturable core   Yoke   Saturable core

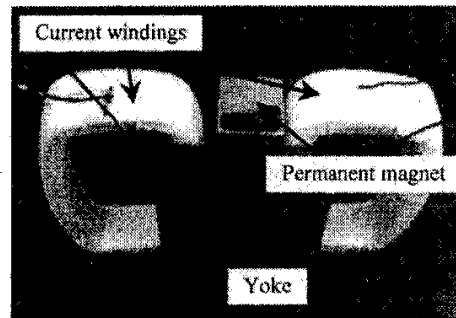Fig. 3. FCL scheme based on parallel biasing mode.

Fig. 4. Experimental model of FCL in parallel biasing mode.

Fig. 3 and a picture of the experimental device is shown in Fig. 4 [4].

(ii) Based on core material

The characteristics of the core material have a strong influence on the performance of the magnetic current limiter. The core should have a rectangular B-H characteristic with a hysteresis loss that is low at the operating frequency. The core can be designed to saturate either by choosing a material with a moderately low saturation flux density or by reducing the core area so that saturation occurs.

Figure 2 shows the fabricated model based on ferrite core in which the cross-section of core is same to that of magnet. Since the saturation flux-density of the Si-steel core is higher than the remnant flux-density of the permanent magnet and the peak flux-density generated by the winding current, the core will never be forced into saturation under normal operating condition. So to implement this type of core, a part of the area of the core has to be reduced. Figure 5 shows the schematic of a half assembly of a magnetic current limiter based on a Si-steel core whose a part of the crosssection has been reduced. The saturation flux density of the steel core (Section #1) is larger than the total of the remnant flux density of the permanent magnet and the peak flux-density generated by the winding current. Consequently, Section #1 will never be forced into saturation. Section #2 having a smaller area compared to the permanent magnet operates in saturation under normal condition and comes out of saturation under fault condition. Figure 6 shows the experimental prototype of a half-assembly of magnetic current limiter based on a steel core. The section of the reduced area is being covered by the winding and is not visible.

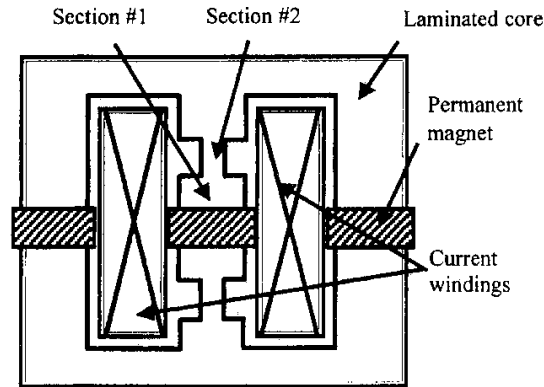To design magnetic current limiter with a low saturation flux-density material, the saturable core is

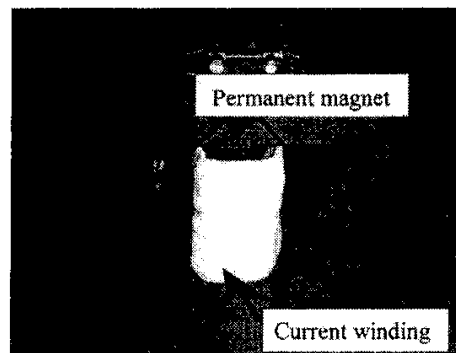Fig. 5. FCL scheme based on Si-steel core.

Fig. 6. Experimental model based on Si-steel core.

constructed in the form of a section of material with a low saturation flux density and a relatively large unsaturated magnetic permeability. Ferrite materials or specially designed amorphous materials can be used.

(iii) Based on the number of phases in the supply system

In multi-phase systems, there are two choices: either to use one three-phase limiter or to use three single-phase limiters. In the three-phase limiter, all closed cores are arranged in a symmetrical fashion along a circle with the three cores sharing a common ring type magnet. For instance in a three-phase system, the cores would be displaced at 120 degrees with respect to one another around the ring-magnet. A schematic depiction of this approach is shown in Fig. 7 and an experimental prototype of a bipolar current limiter is shown in Fig. 8. The core is constructed of a ferrite material [5].

3. Simulation results

The performance of the magnetic current limiter has been simulated by using the tableau approach which is suited for solving transient response problems in coupled electric and magnetic circuits [6,7].
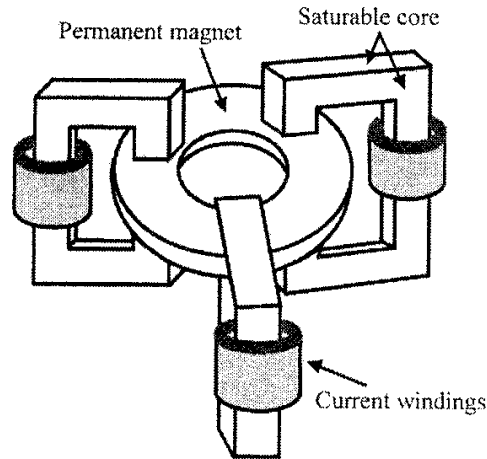
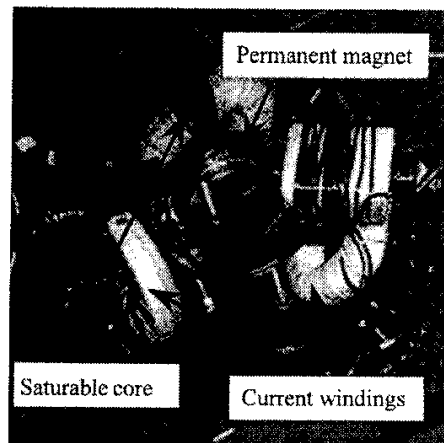Fig. 7. FCL scheme for three-phase applications.

Fig. 8. Experimental model for three-phase applications.

Figure 9 shows the simple circuit used for the analysis of the models used in single-phase supply system and Fig. 10 shows the circuit arrangement used for the performance evaluation for the three-phase model. To simulate the performance of magnetic current limiter using tableau approach, the electromagnetic circuit equations consisting of electrical circuit equations, magnetic circuit equations and eddy-current equations are arranged in a matrix form and are solved by Newton-Raphson and Gaussian eliminations method. The details of the method of solution have been described in [2–5].

Figure 11 shows a comparison of the simulation and experimental results for a typical operating condition for the ferrite core based fabricated model to be used in single-phase system. The fault is simulated by short-circuiting the load resistance with switch "SW". It is observed that the simulation and experimental results are in close agreement to each other. It is also observed that there are blips in the experimental voltage waveform across the limiter even under normal operating condition. The
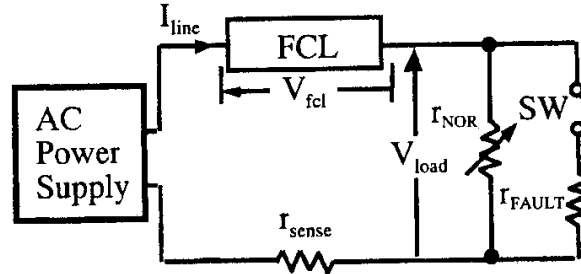
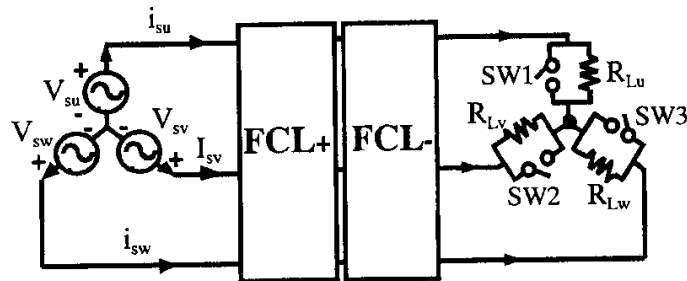Fig. 9. Experimental set-up for a single-phase model.

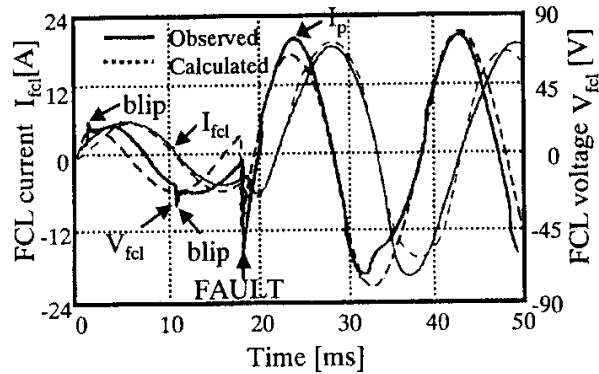Fig. 10. Experimental set-up for a three-phase model.

Fig. 11. Comparison of simulated and experimental results.

discrepancy between the observed results and the simulation results can be attributed to a nonuniform flux distribution in the core. This effect is not possible to take into account in the lumped circuit model.

The performance of a limiter for three-phase supply system with the design specifications of 100 V, 3-ϕ, 60 Hz and a nominal current of 10 A has been simulated using tableau approach. Figure 12 shows the variation of rms voltage across one phase of the limiter as a function of rms current through it. It is observed that the slope changes when the current exceeds 12 A. Figures 13 and 14 show the transient
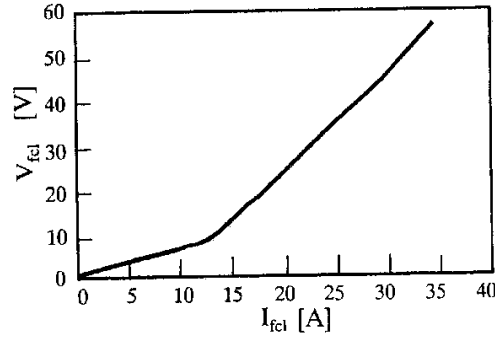
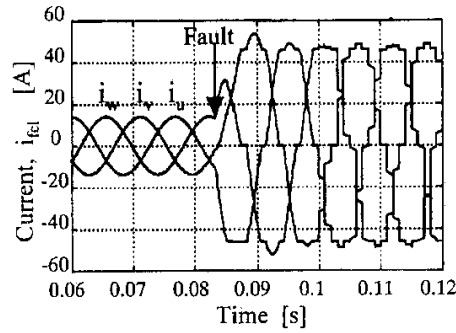Fig. 12. Simulated volt-current characteristic for three-phase model.

Fig. 13. Simulated current waveforms at typical operating condition.
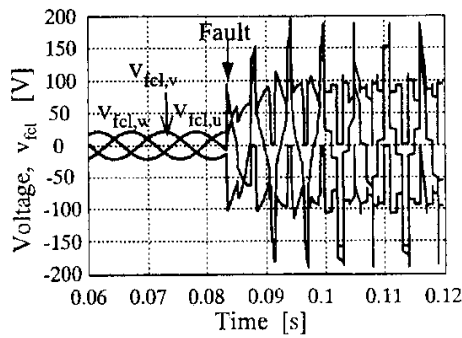

Fig. 14. Simulated voltage waveforms at typical operating condition.

current waveforms and the voltages across the three phases of the limiter for a typical fault condition. The distortion of the waveforms after the fault is due to the swing of the operating flux density of the core from the saturated state to the unsaturated state. In the simulation, the B-H characteristic of the core is represented by two straight lines; one representing the saturated region with a magnetic permeability of μ_s and the other representing the unsaturated condition with a magnetic permeability of μ_u.
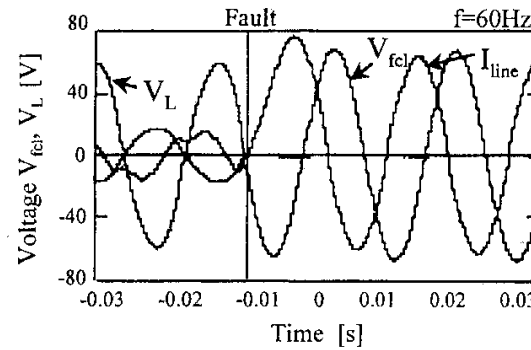
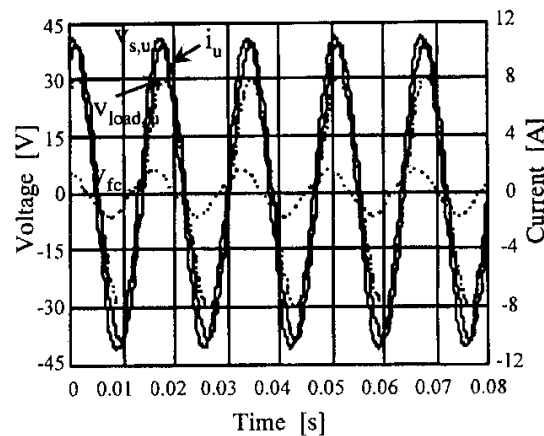Fig. 15. Transient waveforms at a typical operating condition.

Fig. 16. Experimental waveforms at normal operating condition.

4. Experimental results

The experiments for single-phase studies have been carried out on the fabricated models by using the circuit as shown in Fig. 9. Figure 15 shows the transient waveforms for the voltage across the FCL, line current and load voltage for a typical fault. A parallel biased scheme is used in this example.

Experiments for the three-phase model have been carried out by using the circuit shown in Fig. 10. Figure 16 shows the experimental waveforms corresponding to the source voltage, current through the limiter, voltage across the limiter and load voltage of the u-phase under normal operating conditions. Figure 17 shows the three- phase current waveforms and the voltage across the u-phase under a three-phase fault condition. The fault was initiated by closing the switches SW1 to SW3. The current increases considerably compared to the normal operating current but is smaller in comparison to the observed peak current in the absence of the limiter. The differences in the peak fault current values in the three phases may be due to the switching angle of the fault and the nonlinear coupled behavior of the limiter.

The application of a series type of fault current limiter for the protection of power semiconductor devices in moderately low voltage power electronics system has been investigated. Figure 18 shows
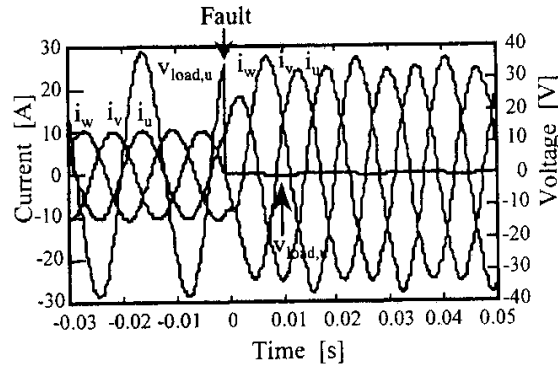
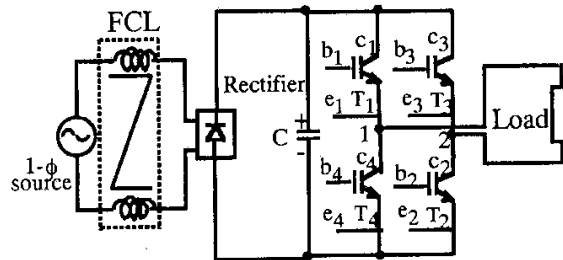Fig. 17. Experimental waveforms at a fault condition.

Fig. 18. Use of a FCL in a power electronics system.

a scheme in which a FCL can be used to limit the peak current in the diode bridge in the event of a short-circuited diode or a short-circuit downstream of the diode bridge. The latter condition will occur when the dc link capacitor is initially charged from a discharged state or if the capacitor is shorted.

Due to the limitation of our set-up, a low voltage scheme has been considered. The specification of the system is: Single-phase 60 Vrms.; 60 Hz, 30 A (nominal peak current); a maximum per-unit reactance of 10% under nominal conditions; typically this number should be very low unless we are dealing with an inverter. The peak value of the fault current should not exceed 200% of the nominal peak current. The following components were used: diodes, Toshiba 12CD12; capacitor, 5000 μF, load resistance 187.5 Ω.

The experiment of charging the capacitor from an initially discharged state was conducted. The line current and voltage across the capacitor were recorded with and without the FCL in the circuit. The corresponding waveforms are shown in Fig. 19. It is seen that the peak starting current reaches nearly 95 A in the absence of the FCL. In contrast, the peak current with the FCL in the circuit is 55 A. This is less than 200% of the nominal peak current.

5. Conclusions

In this paper, the different ways of configuring a passive magnetic current limiter have been described. Simulation results using tableau approach and experimental results for small-scale laboratory based fabricated models have been reported. This type of a fault current limiter can be designed for the
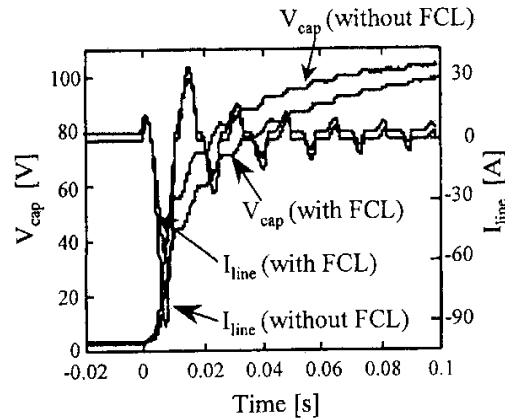
Fig. 19. Charging currents with and without the use of a FCL.

protection of power electronics devices in moderately low voltage power systems. An input rectifier followed by a dc link capacitor and equivalent load has been considered for design purposes. Future development with better magnetic material (rectangular B-H characteristics with a very low saturation flux-density magnetic core) can result in an improved performance.

References

[1]   B.P. Raju, K.C. Parton and T.C. Bartram, A Current Limiting Device using Superconducting D.C. Bias Applications and Prospects, *IEEE Trans. on Power Apparatus and Systems* **101**(9) (1982), 3173–3177.

[2]   S.C. Mukhopadhyay, F.P. Dawson, M. Iwahara and S. Yamada, Analysis, Design and Experimental Results for a Passive Current Limiting Device, *IEE Proceeding on Electric Power Applications* **146**(3) (1999), 309–316.

[3]   S.C. Mukhopadhyay, M. Iwahara, S. Yamada and F.P. Dawson, Investigation of the Performances of a Permanent Magnet Biased Fault Current Limiter Using Steel Core, *IEEE Trans. on Magnetics* **34**(4) (1998), 2150–2152.

[4]   M. Iwahara, S.C. Mukhopadhyay, S. Yamada and F.P. Dawson, Development of Passive Fault Current Limiter in Parallel Biasing Mode, *IEEE Trans. on Magnetics* **35**(5) (1999), 3523–3525.

[5]   S.C. Mukhopadhyay, F.P. Dawson, M. Iwahara and S. Yamada, A Novel Compact Magnetic Current Limiter for Three Phase applications, *IEEE Trans. on Magnetics* **36**(5) (2000), 3568–3570.

[6]   M. Iwahara and E. Miyazawa, A Numerical Method for Calculation of Electromagnetic Circuits Using the Tableau Approach, *IEEE Trans. on Magnetics* **19**(6) (1983), 2457–2460.

[7]   J. Vlack and K. Singhal, Computer Methods for Circuit Analysis and Design, Van Nostrand Reinhold, Electrical and Computer Engineering Series, 1983.